Title
Enhancing Biohybrid CO2 to Multicarbon Reduction via Adapted Whole-Cell Catalysts

Journal
Nano Letters, 22(13)

ISSN
1530-6984

Authors
Kim, Jimin
Cestellos-Blanco, Stefano
Shen, Yue-xiao
et al.

Publication Date
2022-07-13

DOI
10.1021/acs.nanolett.2c01576

Peer reviewed

Supplementary Information for

Enhancing biohybrid CO_2 to multicarbon reduction via adapted whole-cell catalysts

Authors:

Jimin Kim[1,2], Stefano Cestellos-Blanco[1,2], Yue-xiao Shen[3,4], Rong Cai[3], Peidong Yang[1,2,3,5,6*]

Affiliations:

[1] Department of Materials Science and Engineering, University of California, Berkeley, CA 94720, USA.

[2] Center for the Utilization of Biological Engineering in Space (CUBES), Berkeley, CA 94720, USA.

[3] Department of Chemistry, University of California, Berkeley, CA 94720, USA.

[4] Department of Civil, Environmental and Construction Engineering, Texas Tech University, Lubbock, TX 79409, USA.

[5] Materials Sciences Division, Lawrence Berkeley National Laboratory, Berkeley, CA 94720, USA.

[6] Kavli Energy Nanoscience Institute, Berkeley, CA 94720, USA.

[*] To whom correspondence should be addressed. Email: p_yang@berkeley.edu

METHODS

Methanol adaptation of S. ovata. *S. ovata* (DSM 2662) was purchased from the American Type Culture Collection (ATCC). An inoculum of *S. ovata* was grown in DSMZ 311 medium (resazurin omitted; yeast extract added) under strict anaerobic conditions supplemented with betaine as a carbon source, as previous work described.[1,2] Balch-type anaerobic culture tubes with butyl stoppers were employed to maintain a strict anaerobic environment. The adaptive laboratory evolution for methanol adaptation of *S. ovata* was followed by the method introduced by Tremblay *et al*.[3] A 2% of betaine-grown *S. ovata* inoculum was transferred into in an organic DSMZ 311 medium (casitone and resazurin omitted) containing 2% methanol with 80% N_2/20% CO_2 headspace at 20 PSI. This transfer was regarded as the first transfer of ALE. Once *S. ovata* bacteria grow, 10% of the first transfer inoculum at OD_{545} of ~0.1 was transferred to the 2% methanol containing inorganic media. The transfer was repeated 18 times until there was no significant increasement in the growth rate. Exponential doubling rates were calculated as the slope of the least-squares linear fit to log2 (OD_{545}(t)) between exponential phases. Multiple species of heterotroph could potentially grow in the acetate-rich medium, and thus we periodically checked a contamination by 16s rRNA gene sequencing. Each inoculum of 4^{th}, 9^{th}, 18^{th} transfer was collected and the genomic DNA was extracted with Monarch Genomic DNA Purification Kit (New England Biolabs, Ipswich, MA) to identify the purity of the cultures by 16s rRNA gene sequencing. The primer pair of 341F and 1391R were purchased from IDT (USA) and the 16s rRNA gene region was amplified using Q5 High-Fidelity DNA polymerase (New England Biolabs, Ipswich, MA) with MiniAmp thermal cycler (Applied biosystem, Waltham, MA). Sanger sequencing (UC Berkeley DNA sequencing facility, Berkeley, CA) was used to sequence the 16s rRNA gene. The obtained sequences were compared against the NCBI GenBank DNA database using BLAST, and all of 16s rRNA genes of the cultures showed over 98% of identity to *S. ovata* from the NCBI blast results, validating that no contamination occurred during the transfers of ALE. The adapted strains were stored as aliquots at -80 with 10% DMSO as a cryoprotectant.

Whole Genome Sequencing. The 18^{th} transfer was streaked on inorganic agar plates containing 2% methanol. The single colonies of adapted S. ovata were isolated to verify genomic mutations of adapted *S. ovata* using whole genome sequencing (QB3 GSL, Berkeley, CA). Five isolated clones were grown in methanol independently, and the fastest-growing colony was used for 16s rRNA sequencing and whole-genome sequencing (Fig. 1b). The genomic libraries were prepared with Kapa Biosystems library preparation kits (Roche molecular systems, Pleasanton, CA). Briefly, 500 ng of genomic DNA diluted in 50 µl EDTA-free buffer was fragmented with a Covaris-S2 (Woburn, MA). The ends of fragmented DNA were repaired by T4 DNA polymerase, Klenow DNA polymerase, and T4 polynucleotide kinase. The Klenow Exo Minus enzyme was then used to add an ′A′ base to the 3′ end of the DNA fragments. After ligation of the adapters, DNA fragments ranging from 300 to 400 bp were recovered by beads purification. The adapter-modified DNA fragments were enriched by three cycles-PCR. The average size of dsDNA fragments in the libraries was determined with an Agilent 2100 Bioanalyzer. Sequencing was done with a MiSeq Reagent kit v2 (300 cycles) on a NovaSeq (Illumina) platform with a paired-end protocol and read lengths of 151 nucleotides. The genetic analysis was performed using the Geneious 11.1.2 software (https://www.geneious.com).[4] The sequencing reads were then trimmed before being used for variant calling with Geneious variant caller. Poor quality data were trimmed from the ends of the paired reads with an error probability limit of 0.05. Paired reads were then mapped to the reference genome using bowtie2 mapper[5] and set to high

sensitivity resulting in the assembly of the genome on seven contigs. All the samples had average coverage of at least 30X. The reference genome for the analysis was *Sporomusa ovata* DSM 2662 (NCBI accession ASXP00000000.1). Variant calling was performed on the assembled contigs using the Geneious variant finder tool with the following settings: variations positions must be covered by at least 30 reads with a frequency above 0.3. The variant P-value and the strand-bias P-value limits were set to 10^{-5}.

Preparation of p^+ Si nanowire array electrode. The following steps of nanofabrication were carried out with the equipment in Berkeley Marvell nanolab. p^+ Si nanowire arrays were fabricated using reactive-ion etching of patterned single-crystalline Si wafers.[6] The 6-inch p^+-Si (boron) wafers (ρ ~0.001-0.005 Ωcm) were obtained from Addison Engineering, Inc. After thoroughly cleaning in piranha and buffered hydrofluoric acid (BHF), the wafers were patterned with a photoresist dot array using a standard photolithography stepper. Then the wafers underwent inductive-coupled plasma deep reactive-ion etching (Surface Technology Systems. Newport, United Kingdom) to yield uniform nanowire arrays (~20 μm long and ~700 nm in diameter). The Si nanowire arrays were thermally oxidized at 1,000 ºC for 3 hours, followed by etching in BHF for at least 5 minutes. The resulting thinned-down Si nanowires (700-800 nm in diameter) were subsequently coated with 5 nm of TiO_2 protective layer by atomic layer deposition (Picosun ALD) to maintain stable performance in a near neutral pH electrolyte for an extended period. To facilitate the electron transfer from the cathode to the bacterium *S. ovata*[7], ~10 nm nickel (Ni) was sputtered on the surface of the Si nanowire arrays (Edwards Vacuum Inc, San jose, CA). For the electrode fabrication, ohmic contact to the device chip was made by rubbing Ga-In eutectic on its backside with a diamond-tipped scribe. Then the chip was fixed on Ti foil with conductive silver paint and carbon tape, resulting in good electrical connections. After that, the Si nanowire array samples were sealed using a nail polish, and the electrodes were ready for electrochemical characterizations.

Electrochemical characterization. All electrochemical measurements were carried out using a home-built electrochemical setup. The setup is a two-chamber cell, with a working electrode and a reference electrode (Ag/AgCl, 1M KCl, CH Instruments, Kwun Tong, Hong Kong) in one chamber and a Pt wire as a counter electrode in the other chamber. The working electrode is sealed with an O-ring with a contact area of 1.2 cm^2. A gas inlet and a outlet are imbedded for the purpose of gas purging. The two chambers were separated by an anion-exchange membrane (AMI-7001S, Membranes International, Ringwood, NJ). All the electrochemical characterization was performed using Gamry Interface 1000 potentiostats (Gamry Instrument, Warminster, PA). $FE_{acetate}$ and J_{aceate} were both characterized vs *SHE* defined as following:

$$\text{V vs } SHE \text{ (V)} = \text{V } vs. \text{ Ag/AgCl (V)} + 0.209 \text{ (V)}$$

The nanowire-bacteria hybrids were formed in the cathodic chamber using the phosphate-enhanced inorganic medium as an electrolyte as previous work described.[1] The initial pH value of the electrolyte was adjusted to 6.4 by adding a 1% of hydrochloric acid and confirmed with a digital pH meter (Mettler Toledo, Columbus, OH). 15 ml and 30 ml of the pH-adjusted electrolyte were introduced to the cathodic and anodic side of the electrochemical cell, respectively. We ran abiotic chronoamperometry (-0.8 V vs *SHE*) for 24 hours with 80% N_2/10% H_2/10% CO_2 gas bubbling to remove O_2 residue in the cathode chamber. Prior to the chronoamperometry experiments, both WT and adapted strains were equally precultured twice in DSMZ 311 medium (betaine, casitone and

resazurin omitted; yeast extract added) with hydrogen as the electron donor (80% H_2 and 20% CO_2) to help upregulate their electron-bifurcating hydrogenase and to stimulate the subsequent productions of electron carriers. The hydrogen-grown *S. ovata* cells were then inoculated into the cathodic chamber to make the final OD_{545} of ~0.08. After bacteria inoculation, the electrochemical bias was kept at -0.6 V vs *SHE*, and the dispersion was cultured under the same 80% N_2/10% H_2/10% CO_2 gas environment for a day. The gas was then switched to 80% N_2/20% CO_2 and the bias was kept at -0.6 V vs *SHE*. The Si nanowire electrode served as a sole electron source for the growth of bacteria. The current increased ~30 μA after switching the gas, possibly due to the absence of purged hydrogen gas. After 24-hour incubation on the poised electrode and under 80% N_2/20% CO_2, half of the electrolyte in the cathode chamber was replaced with a new electrolyte. After another 24 hours, the cathodic electrolyte was replaced again, and the electrolyte became clear (<0.03 OD_{545}) as most bacteria settled on the SiNWs array and a stable bacteria-nanowire hybrid was achieved. Then, the hybrids were ready for the electrochemical acetate production as follows. Starting from less negative overpotential, 0.7 V vs *SHE*, chronoamperometry was run for at least 6 hours at each electrochemical bias. After one chronoamperometry cycle was complete, an aliquot of the medium was sampled, and the same amount of fresh medium was injected into the electrochemical cell to the volume constant. After the series of acetate production experiments, the hybrids are characterized with electrochemical impedance spectroscopy (EIS) to verify the charge transfer resistances between cathodes and biofilm at multiple potentials. EIS was performed with a stimulus of 10 mV peak-to-peak on a -0.6 V vs. Ag/AgCl in the frequency range from 1 MHz to 0.1 Hz.

Analysis of acetate production. Aliquots were obtained from the cathode chamber and the anode chamber for acetate production analysis. Acetate concentration of the sample was quantified by proton nuclear magnetic resonance (^{1}H-qNMR) spectroscopy with sodium 3-(trimethylsilyl)-2,2',3,3'-tetradeuteropropionate (TMSP-d4) as the internal standard. After obtaining the acetate concentration of each sample, $FE_{acetate}$ is calculated based on following equation:

$$FE_{acetate} = \frac{96485 \times 8 \times \text{incremental mole of acetic acid}}{\int Idt}$$

And the specific CO_2-reducing current density $J_{acetate}$ is defined as:

$$J_{acetate} = FE_{acetate} \times J_{total}$$

where J_{total} is the total current density during chronoamperometry.

Scanning electron microscopy (SEM) characterization. After the electrochemical characterizations were complete, the nanowire-bacteria hybrids were subjected to SEM characterization. First, an overnight bacteria fixation was performed by adding 2.5% glutaraldehyde directly to the medium in the cathode chamber. Then the electrodes were washed with DI water followed by dehydration in increasing concentrations of ethanol (12.5%, 25%, 37.5%, 50%, 62.5%, 75%, 87.5%, 100%, 10 minutes each). Prior to imaging, the electrodes were cleaved along the middle and then sputtered with ~5 nm of Au (Denton Vacuum, Moorestown, NJ). The nanowire-bacteria hybrids were imaged at 5 keV/12 μA by field emission SEM (JEOL FSM6430, Tokyo, Japan) and at 15kV/ high probe current by Benchtop SEM (JCM-7000, Tokyo, Japan). The SEM images showed a clear bio-inorganic interface and the density of *S. ovata* could be estimated from the SEM characterization (Fig.S3). The cell density

of the close-packed biohybrid was calculated by counting the number of cells per one nanowire within given areas of SEM images, as previous work described.[1] The cell density per nanowire was used to calculate single-cell TOR of each system based on following equation:

$$TOR_{e^-} = \frac{J_{acetate} \times A_{NW} \times N_A}{96485 \times 8 \times Cell\ density}$$

where $J_{acetate}$ is the CO_2-reducing current density during chronoamperometry, A_{NW} is the unit area of a nanowire, 4 μm2/wire, N_A is the Avogadro's number and cell density is the number of bacterial cells attached to a nanowire.

For the hydrogen grown *S. ovata*, TOR of each system was calculated based on following equation:

$$TOR_{H_2} = \frac{Daily\ acetate\ production\ rate \times N_A}{OD_{545} \times 8.0 \times 10^8 \times 24 \times 3600}$$

where N_A is the Avogadro's number. In this calculation, we assume 1.0 of OD corresponds to ~ 8×10^8 cells/mL, which is the value for *E. coli*.

Cell binding quantification. EIS was used to quantify the attachment of *S. ovata* on the Si NWs electrode surfaces based on the reported work by Ariel *et al*.[8] The electrolyte for the EIS contained 4 mM of MV and MV^{2+} in the phosphate-enhanced inorganic medium, which was used for the chronoamperometry experiment. Electrochemical measurements were acquired at the open circuit potential (OCP) of the cathode and the OCP was measured for 60 s prior to EIS. EIS measurements were conducted from 1 MHz to 0.1 Hz with 10 points per decade and a 10 mV AC voltage. Electrochemical data analysis, including circuit modeling, was performed using the Gamry Echem Analyst software. Charge transfer resistance (RCT) was derived from a constant phase element (CPE) with diffusion circuit model fit.

Gene	Annotation	Position	Mutation	Function
SOV_1C00290	type II asparaginase	508	GCC -> ACC	
SOV_1c01720	glycosyltransferase family protein	320	CCT -> CTT	
SOV_1c02350	glycosyltransferase family 4 protein	408	G deletion	
SOV_1c05650	tungsten-containing aldehyde ferredoxin oxidoreductase	1618	GCT -> ACT	Ethanol production
SOV_1c05700	sigma-54-dependent Fis family transcriptional regulator	448	A insertion	Regulation
SOV_1c05920	Adenine DNA glycosylase MutY	836	GAG -> GGG	
SOV_1c05960	(Fe-S)-binding protein	316	A deletion	
SOV_1c06360	5,10-methylenetetrahydrofolate reductase MetF	206	A deletion	Central Metabolism
SOV_1c06480	hypothetical protein	16	A insertion	
SOV_1c07740	NADH-quinone oxidoreductase subunit E NuoE	394	GTT -> ATT	Central metabolism
SOV_1c10930	**acetate/propionate family kinase AckA**	**748**	**ACT -> GCT**	**Central Metabolism**
SOV_2c00410	**FeMo cofactor biosynthesis protein NifB1**	**847**	**GCC -> ACC**	**Nitrogen fixation**
SOV_2c04150	**sigma-54-dependent Fis family transcriptional regulator**	**1253**	**C deletion**	**Regulation**
SOV_2c05810	homocysteine S-methyltransferase family protein	1933	GCT -> ACT	
SOV_2c06570	hydrogenase maturation nickel metallochaperone HypA	21	GCG -> GCA	
SOV_2c06550	D-alanyl-D-alanine carboxypeptidase	923	GTT -> GCT	
SOV_2c09560	2-C-methyl-D-erythritol 4-phosphate cytidylyltransferase	655	GCT -> ACT	
SOV_2c10690	DUF3383 family protein	572	CCG -> CGG	
SOV_2c11610	molybdopterin-dependent oxidoreductase	605	GCC -> GTC	
SOV_2c11670	Cytochrome c biogenesis protein CcsA	2041	C -> T	
SOV_3c00460	**methanol--corrinoid protein Co-methyltransferase**	**382**	**GGC -> AGC**	**Central metabolism**
SOV_3c01630	Protein-export membrane protein SecG	186	TCA -> TCG	
SOV_3c08160	**diguanylate cyclase DosC**	**251**	**A deletion**	**Regulation**
SOV_3c08430	**diguanylate cyclase DosC**	**1822**	**GTT -> ATT**	**Regulation**
SOV_3c08810	class I SAM-dependent methyltransferase	280	A deletion	
SOV_4c01810	Anti-sigma F factor antagonist SpoIIAA	285	ATG -> ATA	
SOV_5c01480	EAL domain-containing protein	285	T deletion	
SOV_5c02520	hypothetical protein	41	T deletion	

SOV_6c01260	DUF2460 domain-containing protein	397	AGC -> GGT

Table S1. Mutations found in a single colony isolated from the 18th transfer culture with 2% methanol. The mutations in bold are found in the same encoding genes as the previous report by Trembley *et al*.[3]

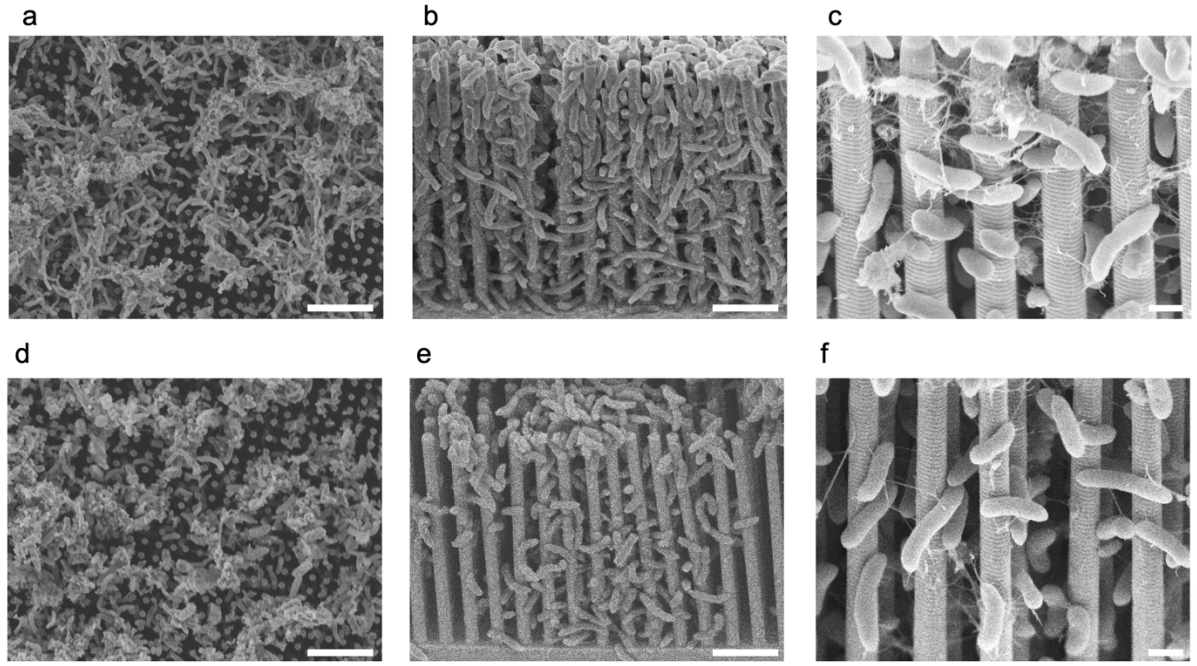

Figure S1. A representative SEM image of the nanowire-bacteria hybrid system using methanol-adapted *S. ovata* (a-c) and wild-type *S. ovata* (d-f). SEM images were obtained after the set of chronoamperometry experiments. The images showed that the close-packed nanowire-bacteria biohybrids were still maintained after the operation. The cell density of the close-packed hybrids could be estimated by counting the number of cells within the given areas of SEM images along the nanowire. The resulting bacteria loading density was ~13 and ~12 per nanowire, respectively. The scale bar is 5 μm (a,b,d, and e) and 1 μm (c and f), respectively.

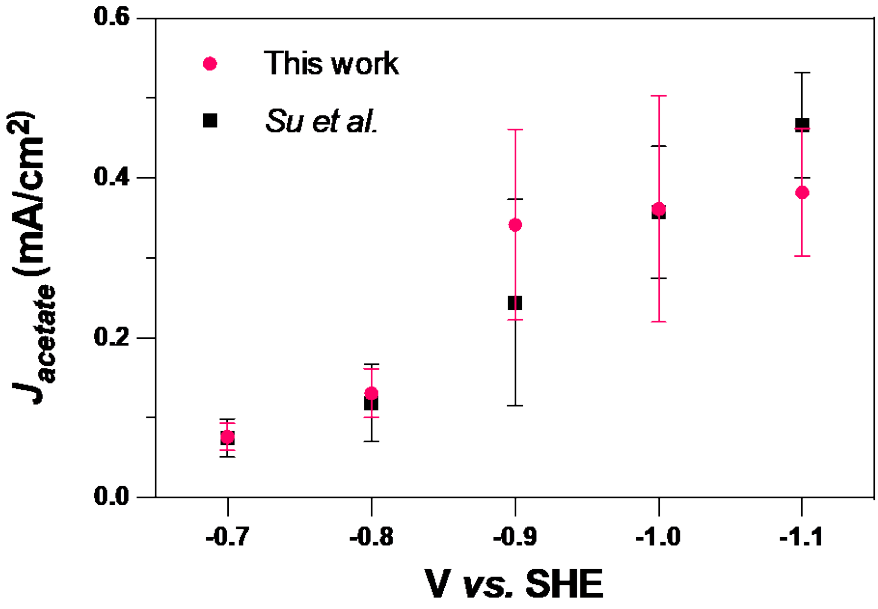

Figure S2. Comparison in CO_2-reducing current densities ($J_{acetate}$) for the close-packed nanowire-bacteria hybrids with the wild-type *S. ovata* in this work and the previous work by Su *et al*. The established inorganic phosphate-buffered media with pH 6.4 was used (n = 3 for each case).

Organism	**Feedstock**	**Electron consumption rate ($\mu mol\ e^- \cdot s^{-1} \cdot$ gDCW^{-1})**	**Feedstock consumed (mM)**	**Acetate formed (mM)**	**Acetate production rate ($\mu mol\ e^- \cdot s^{-1} \cdot$ gDCW^{-1})**	**TOR (acetate molecules · s^{-1} · cell^{-1})**
Clostridium thermoaceticum	H_2	33	77.5	19.1	33	1.4×10^6
Acetogenium kivui	H_2	157			157	6.9×10^6
Treponema primitia, ZAS-2	H_2	40	5.23	1.23	37	7×10^6
Treponema primitia, ZAS-1	H_2	148			148	6.5×10^6
Acetonema longum	H_2	11	100	22.7	10	4.4×10^6
Acetobacterium Woodii	H_2	8	1	0.22	7	3.1×10^6
Eubacterium limosum	Methanol	22			22	1.0×10^6
Sporomusa termitida	Methanol	16	100	75.7	16	0.7×10^6

Table S2. Inherent TOR values of acetogenesis converted from reported electron consumption rates of multiple species of acetogens. The reported electron consumption rates[9] were converted into the acetate production rates (in a unit of $e^- \cdot s^{-1} \cdot$gDCW^{-1}) based on the ratio of feedstock consumed and acetate formed. If the two values were not provided, 100% conversion efficiency from electron to acetate was assumed. The calculated acetate production rates were then converted into the TOR values assuming that OD_{600} 1.0 corresponds to $\sim 8 \times 10^8$ cells/mL and 0.47 gDCW/L, which are the reported values for *E. coli*[10], and a unit cellular dry cell weight of 5.87510^{-13} gDCW was used for the calculation of single-cell TOR values of acetogens.

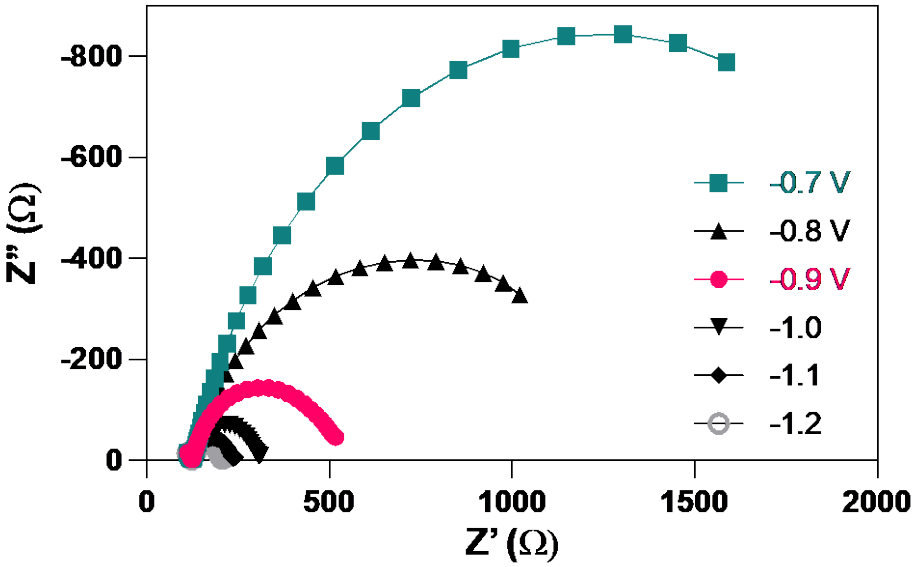

Figure S3. Nyquist impedance plots of the biohybrids using methanol-adapted strain. Each data was fitted to the model circuit shown in Fig. 4b and the results of the fits are listed in Supplementary Table 3.

	Wild-type *S. ovata*	**Methanol adapted *S. ovata***
$\mathbf{R_s}$	83.14 ± 0.432	123.5 ± 0.606
R_{ct}	581 ± 34.05	309.9 ± 32.43
$R_{biofilm}$	861.1 ± 9.385	370.9 ± 14.65
Goodness of Fit	6.53×10^{-3}	2.50×10^{-3}

Table S3. Fits to the EIS data (Fig. S3) of biohybrids using wild-type *S. ovat*a and methanol adapted *S. ovata* at -0.9 V vs *SHE* using a typical equivalent circuit (shown in Fig. 4b) for bioelectrochemical systems.[7,11]

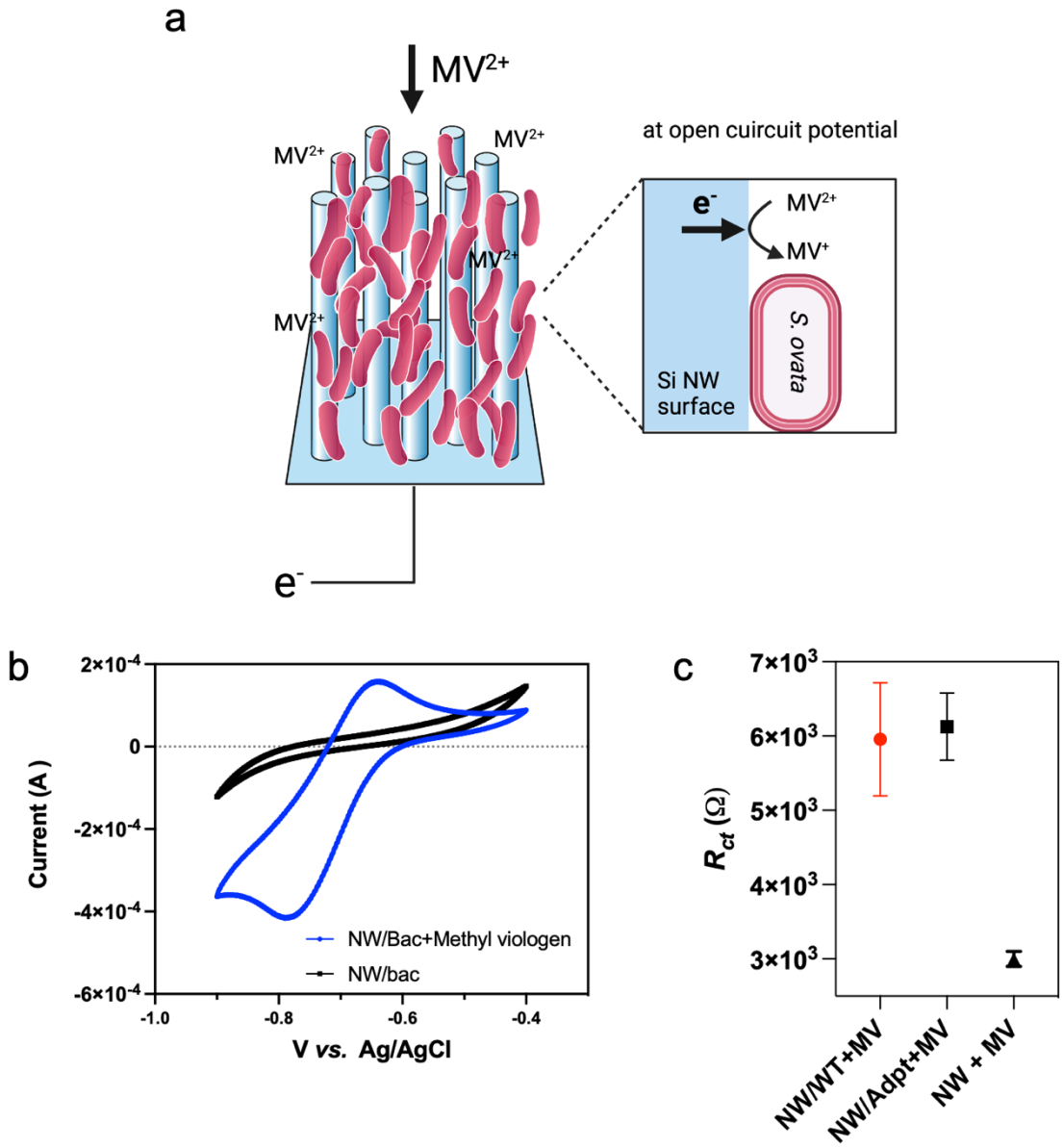

Figure S4. Relative cell binding quantification. a, Illustration of the cell binding characterization using methyl viologen (MV) as an electron acceptor. **b,** Subsequent CV scans before and after the addition of methyl viologens in the electrolyte **c,** Extracted charge transfer resistance values from the EIS data of the two biohybrid systems using wild-type (NW/WT+MV), methanol adapted (NW/Adpt+MV) strains, and abiotic system (NW + MV) using a constant phase element (CPE) with diffusion circuit model fit.

References

(1) Su, Y.; Cestellos-Blanco, S.; Kim, J. M.; Shen, Y. xiao; Kong, Q.; Lu, D.; Liu, C.; Zhang, H.; Cao, Y.; Yang, P. Close-Packed Nanowire-Bacteria Hybrids for Efficient Solar-Driven CO2 Fixation. *Joule* **2020**, *4* (4), 800–811. https://doi.org/10.1016/j.joule.2020.03.001.

(2) Cestellos-Blanco, S.; Friedline, S.; Sander, K. B.; Abel, A. J.; Kim, J. M.; Clark, D. S.; Arkin, A. P.; Yang, P. Production of PHB From CO2-Derived Acetate With Minimal Processing Assessed for Space Biomanufacturing. *Front. Microbiol.* **2021**, *12* (July), 1–12. https://doi.org/10.3389/fmicb.2021.700010.

(3) Tremblay, P. L.; Höglund, D.; Koza, A.; Bonde, I.; Zhang, T. Adaptation of the Autotrophic Acetogen Sporomusa Ovata to Methanol Accelerates the Conversion of CO2 to Organic Products. *Sci. Rep.* **2015**, *5* (November), 1–11. https://doi.org/10.1038/srep16168.

(4) Sevestre, F.; Facon, M.; Wattebled, F.; Szydlowski, N. Facilitating Gene Editing in Potato: A Single-Nucleotide Polymorphism (SNP) Map of the Solanum Tuberosum L. Cv. Desiree Genome. *Sci. Rep.* **2020**, *10* (1), 1–8. https://doi.org/10.1038/s41598-020-58985-6.

(5) Langmead, B.; Salzberg, S. L. Fast Gapped-Read Alignment with Bowtie 2. *Nat. Methods* **2012**, *9* (4), 357–359. https://doi.org/10.1038/nmeth.1923.

(6) Liu, C.; Gallagher, J. J.; Sakimoto, K. K.; Nichols, E. M.; Chang, C. J.; Chang, M. C. Y.; Yang, P. Nanowire-Bacteria Hybrids for Unassisted Solar Carbon Dioxide Fixation to Value-Added Chemicals. *Nano Lett.* **2015**, *15* (5), 3634–3639. https://doi.org/10.1021/acs.nanolett.5b01254.

(7) Su, Y. Silicon Nanowires for Solar-to-Fuel Conversion, University of California, Berkeley, 2017.

(8) Furst, A. L.; Smith, M. J.; Lee, M. C.; Francis, M. B. DNA Hybridization to Interface Current-Producing Cells with Electrode Surfaces. *ACS Cent. Sci.* **2018**, *4* (7), 880–884. https://doi.org/10.1021/acscentsci.8b00255.

(9) Claassens, N. J.; Cotton, C. A. R.; Kopljar, D.; Bar-Even, A. Making Quantitative Sense of Electromicrobial Production. *Nat. Catal.* **2019**, *2* (5), 437–447. https://doi.org/10.1038/s41929-019-0272-0.

(10) Glazyrina, J.; Materne, E. M.; Dreher, T.; Storm, D.; Junne, S.; Adams, T.; Greller, G.; Neubauer, P. High Cell Density Cultivation and Recombinant Protein Production with Escherichia Coli in a Rocking-Motion-Type Bioreactor. *Microb. Cell Fact.* **2010**, *9*, 1–11. https://doi.org/10.1186/1475-2859-9-42.

(11) Rengasamy, K.; Ranaivoarisoa, T.; Singh, R.; Bose, A. An Insoluble Iron Complex Coated Cathode Enhances Direct Electron Uptake by Rhodopseudomonas Palustris TIE-1. *Bioelectrochemistry* **2018**, *122*, 164–173. https://doi.org/10.1016/j.bioelechem.2018.03.015.